Pergamon

J. Steroid Biochem. Molec. Biol. Vol. 66, No. 5-6, pp. 281–293, 1998

Printed in Great Britain
PII: S0960-0760(98)00061-2
0960-0760/98 $19.00 + 0.00

In Vivo Metabolism of the Vitamin D Analog, 22-Oxacalcitriol: Evidence for Side-chain Truncation and 17-Hydroxylation

Masaki Ishigai*, Shinichi Arai, Yoshihiko Ishitani and Kenji Kumaki

Drug Metabolism and Pharmacokinetics Laboratory, Chugai Pharmaceutical Co. Ltd., 3-41-8 Takada, Toshima-ku, Tokyo 171, Japan

After intravenous administration of the vitamin D_3 analog, 22-oxacalcitriol (OCT), to normal rats plasma metabolites were investigated by HPLC, GC-MS and LC-MS. Five side-chain oxidation metabolites, 24*R*(OH)OCT, 24*S*(OH)OCT, (25*R*)-26(OH)OCT, (25*S*)-26(OH)OCT and 24oxoOCT, were identified by comparison with the corresponding synthetic compounds. These side-chain oxidation metabolites were similar to those of calcitriol [1α,25$(OH)_2$ vitamin D_3] described previously. Besides these five metabolites, two unique side-chain cleavage metabolites, 20*S*(OH)-hexanor-OCT and 17,20*S*$(OH)_2$-hexanor-OCT, were identified as main metabolites in plasma by GC-MS and LC-MS using a specific chemical reaction. Our studies suggest that OCT is extensively metabolized and circulates in blood as a number of metabolites as well as unchanged OCT. This metabolism includes both unique pathways of C_{23}–O_{22} cleavage and 17-hydroxylation, in addition to the side-chain oxidation metabolites similar to those of 1α,25-$(OH)_2D_3$.

J. Steroid Biochem. Molec. Biol., Vol. 66, No. 5-6, pp. 281–293, 1998

INTRODUCTION

Since 1α,25-dihydroxyvitamin D_3 [1,25-$(OH)_2D_3$] was shown to induce differentiation in myloid leukemia cells in addition to its regulation of calcium and phosphorus metabolism [1], a number of analogs have been synthesized with the aim of separating the differentiating-inducing activity and the potential hypercalcemic action [2–6]. 22-Oxacalcitriol [OCT] was an early analog developed for this purpose [7]. OCT is more potent than 1,25-$(OH)_2D_3$ in inducing differentiation and suppressing the proliferation of human and mouse myeloid leukemia cells [8, 9], but is much less effective in mobilizing calcium from bone and in stimulating intestinal calcium transport in vitamin D-deficient and normal rats [7, 10, 11]. The mechanisms which are responsible for these differences in biological activity remain unclear, but factors such as metabolism and cellular uptake could play a role.

Metabolic studies on OCT have been described mainly using a variety of cultured cell lines, including a bovine parathyroid cell line [12], a human hepatoma cell line and three vitamin D-target cell lines (one rat osteosarcoma cell line and two human keratinocyte cell lines [13]). It has been shown that OCT is metabolized to side-chain oxidation metabolites (SCOMs) and side-chain cleavage metabolites (SCCMs) in these cell cultures. The SCOMs show similar metabolic patterns to 1,25-$(OH)_2D_3$, while the SCCMs have unique structures derived from the original structure of OCT. Metabolic studies in cell culture models have provided good evidence for a preliminary evaluation of the metabolism of 1,25-$(OH)_2D_3$ or its analogues. However, it is difficult to extrapolate to *in vivo* metabolism using this information alone, because some cell cultures exhibit different metabolite and metabolic ability. Moreover, there is little information on the tissues and enzymes involved in the metabolism of an analogue such as OCT. Also, little is known about the *in vivo* metabolism of OCT, except that it appears to be excreted in the bile as a glucuronide conjugate of a derivative of a truncated version of OCT [14, 15].

We have investigated the metabolites in plasma after administration of OCT to rats in order to clarify the *in vivo* metabolism and examine differences in the *in vivo* and *in vitro* metabolism of OCT. This paper

*Correspondence to M. Ishigai.
Received 21 Nov. 1997; accepted 17 Mar. 1998.

reports that OCT is metabolized to the unique metabolite, 17,20*S*(OH)$_2$-hexanor-OCT, as well as the metabolites identified in cell cultures.

MATERIALS AND METHODS

Reagents and materials

OCT, 20*R*(OH)-hexanor-OCT, 20*S*(OH)-hexanor-OCT, 20-oxo-hexanor-OCT, 24*R*(OH)OCT, 24*S*(OH)OCT, (25*R*)-26(OH)OCT, (25*S*)-26(OH)OCT and 24-oxoOCT were synthesised in the Chugai Pharmaceutical Research Laboratory [7, 16, 17]. All substances were >99% pure as determined by HPLC. Tritium (^{3}H) labelled OCT compounds were also synthesized in the Chugai Pharmaceutical Research Laboratory [18]. Since two kinds of radiolabeled OCT were used here, the labeled positions in [^{3}H]OCT are highlighted as [2β-^{3}H]OCT and [26-^{3}H]OCT (Fig. 1). The specific activity of [2β-^{3}H]OCT and [26-^{3}H]OCT was 880 kBq/μg (23.8 μCi/μg) and 6.30 MBq/μg (170 μCi/μg), respectively. Radiochemical purity was more than 98% for each. Tween 20 was obtained from Wako Pure Chemical (Osaka, Japan). Acetonitrile of HPLC grade, ethylacetate, isopropanol, hexane, pyridine and tetrahydrofuran all of analytical grade were purchased from Junsei Chemical (Tokyo, Japan). BondElut NH_2 (1 ml/100 mg) and BondElut DEA (1 ml/100 mg) cartridges and Sylon BFT Kits (trimethylsilylation reagent) were obtained from Varian (Harber City, CA) and Supelco (Bellefonte, OH), respectively. All solvents and reagents used were of the highest commercial grade available.

Animals

Normal male Jcl/SD rats (CLEA Japan, Tokyo, Japan) were purchased at 6–7 weeks of age. All experiments were carried out at an age of 7–9 weeks. There was no special pretreatment of rats before drug administration.

Administration

Two different solutions for the detection of metabolites, [2β-^{3}H]OCT and [26-^{3}H]OCT, were prepared as saline solutions containing 0.01% Tween 20 at a concentration of 10 μg/ml (8.80 MBq/ml). Each solution was administered intravenously to rats at a dose of 10 μg/kg. Another solution of higher concentration for the identification or isolation of metabolites was

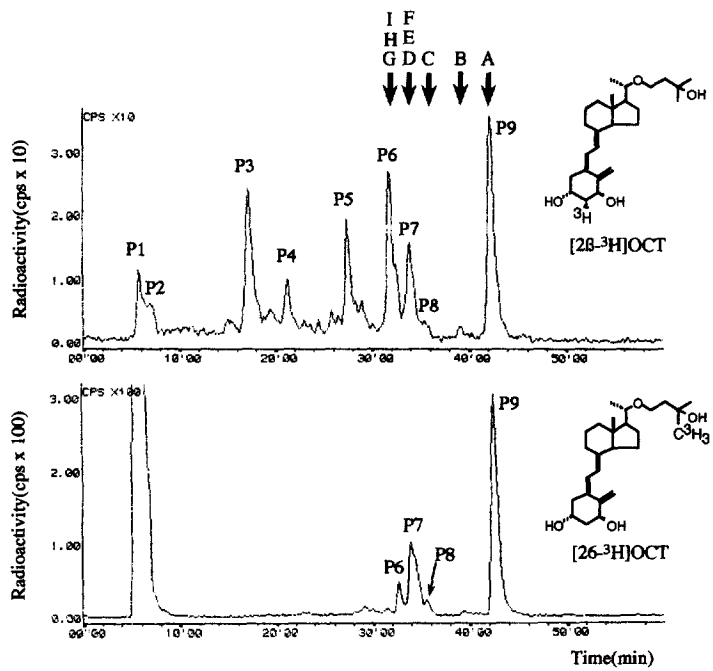

Fig. 1. High performance liquid radio chromatographic profile of plasma metabolites 2 h after administration of [^{3}H]OCT to rats. [^{3}H]OCT labelled at two different positions, [2β-^{3}H]OCT (upper panel) and [26-^{3}H]OCT (lower panel), were administered intravenously at the dose of 10 μg/kg to rats. Arrows (A to I) indicate the retention times of synthetic standards in the same system; (A) OCT, (B) pre-OCT, (C) 24-oxoOCT, (D) 20oxo-hexanor-OCT, (E) 24*S*(OH)OCT, (F) 24*R*(OH)OCT, (G) 20*S*(OH)-hexanor-OCT, (H) (25*R*)-26(OH)OCT and (I) (25*S*)-26(OH)OCT. High performance liquid chromatography was carried out under the following conditions; column: YMC-Pack ODS-A A-313 (6.0 × 250 mm), mobile phase; (A): THF-H_2O (1:9, v/v), (B): THF-CH_3OH-H_2O (2:1:2, v/v/v), [(B): 0% (0 min); 75% (20 min); 75% (50 min); 100% (50.1 min)], flow rate: 1.0 ml/min, detection:radioactivity (CPS).

prepared in the same manner as described above and administered at a final dose of 2 or 25 mg/kg.

Collection and preparation of blood samples

All blood samples were collected 2 h after administration and taken into centrifugation tubes including a drop of heparin. They were centrifuged at 3,000 rpm for 10 min and the supernatant samples were used as plasma. Plasma samples for the detection of metabolites were deproteinated with acetonitrile. The protein-free fractions were concentrated under nitrogen gas and the residue was redissolved in HPLC mobile phase, tetrahydrofuran (THF)–methanol (MeOH)–water (H_2O) (2:1:2, v/v/v). Plasma samples for the detection of metabolites were extracted as described in Section 2.5.

Extraction of plasma metabolites

Extraction of metabolites from plasma prior to GC-MS or LC-MS was carried out as reported previously [19]. Three volumes of ethyl acetate was added to about 10 ml plasma and vigorously mixed. After extraction, the organic layer was evaporated to dryness under nitrogen gas and the residue was redissolved in 200 μl of a mixture of isopropanol (IP)-hexane (HEX) (4:96, v/v). This solution was applied to a BondElut NH_2 cartridge and the column washed with 2 ml of a mixture of IP-HEX (20:80, v/v) and the elute was evaporated to dryness under nitrogen gas.

HPLC

Profiles of metabolites and their purification were obtained using a model SCL-6A control system, model LC-6A pump, a model SPD-2A UV-detector (Shimadzu, Kyoto, Japan) and a model Ramona-5-LS radio-detector (Raytest, FRG). Separation of plasma metabolites after administration of [2β-^{3}H]OCT or [26-^{3}H]OCT was performed on a 5-μm YMC-Pack ODS-A column (6.0 × 250 mm I.D., YMC, Tokyo, Japan) with gradient elution using two mobile phases: A: THF–H_2O (1:9, v/v), B: THF–MeOH–H_2O (2:1:2, v/v/v), [B: 0% (0 min); 75% (20 min); 75% (50 min); 100% (50.1 min)] at a flow rate of 1.0 ml/min.

Separation of non-polar metabolites obtained by extraction of plasma metabolites after administration of OCT was performed on a YMC-Pack ODS-A column (as described in Section 2.5) eluting under isocratic conditions with H_2O–THF–CH_3CN (65:35:2, v/v/v) at a flow rate of 1.0 ml/min. Purification of P5 and P8 was carried out by collecting each peak which corresponded to the t_R of radio-labelled P5 and P8 under the following HPLC conditions. Isolation of P5 was carried out using the same conditions as for the separation of non-polar plasma metabolites except for using a mobile phase of H_2O–CH_3CN (50:50, v/v). Further separations of P6 and P7 were carried out on a Capcell Pak NH_2 column (4.6 × 250 mm I.D., Shiseido, Tokyo, Japan), eluting under isocratic conditions with HEX–IP–MeOH (91:7:2, v/v/v) at a flow rate of 2.5 ml/min.

Periodate oxidation

P5 isolated by HPLC was dissolved in 50 μl methanol and 100 μl ethanol, to which 50 μl aqueous $NaIO_4$ (0.1%, w/v) had been added. The reaction was allowed to proceed for 30 min at 50°C in a shielded tube. The reactant was evaporated to dryness and the residue was redissolved in 50 μl HPLC mobile phase [CH_3CN–H_2O (2:3, v/v)].

GC-MS

GC-MS was performed using a JEOL JMS DX-300 mass spectrometer (Tokyo, Japan) equipped with a DA-5000 data system. Metabolites extracted from plasma were derivatized to their pertrimethylsilyl ethers (TMS) and then analyzed by GC-MS as described previously [19]. GC analysis of vitamin D derivatives such as OCT at a high temperature causes B ring closure producing pyro- and isopyro-isomers [19, 20]. Although two peaks for each compound are basically observed in a total ion chromatogram, only the mass spectra obtained from the first peak (pyro-isomer) are illustrated in the figures because there is little difference between the two. Identification of metabolites was carried out by comparing the t_R and mass spectrum for each metabolite in GC-MS with those of synthesized standard metabolites which have been previously reported [19].

LC-MS

LC-MS was performed using a Finnigan TSQ-700 triple stage quadrupole mass spectrometer (San Jose, CA) fitted with Shiseido NanospacesI-1 equipment (Tokyo, Japan). Purified plasma metabolites (P5 and P8) were analyzed by LC-MS as described previously [19]. Identification of metabolites was carried out as described in Section 2.8.

RESULTS

HPLC of plasma metabolites

The HPLC radio-chromatograms of metabolites in plasma samples collected 2 h after intravenous administration of [2β-^{3}H]OCT or [26-^{3}H]OCT are shown in Fig. 1. More than nine metabolite peaks including unchanged OCT were detected in the chromatograms obtained after administration of [2β-^{3}H]OCT. In contrast, only four main peaks in addition to OCT except for a void volume peak, were observed after administration of [26-^{3}H]OCT. A comparison of both chromatograms showed that three peaks (P7, P8 and part of P6) observed with [2β-^{3}H]OCT were also found with of [26-^{3}H]OCT, and the other peaks (P1,

P2, P3, P4, P5 and the other part of P6) were missing from the [26-^{3}H]OCT chromatogram. These results suggest that the missing peaks are metabolites which have no side-chain moiety. A comparison of the t_R's with several synthesized putative metabolites indicated that peaks P6 and P7 should contain at least two different metabolites.

Non-polar plasma metabolites (P5, P6, P7 and P8) were shown to be extracted effectively by ethyl acetate, but polar metabolites (P1, P2, P3 and P4) were not. The HPLC profile of the extract of plasma metabolites after administration of unlabelled OCT at a high dose (2 and 25 mg/kg), was shown to be similar to that obtained from the extract of metabolites after administration of [2β-^{3}H]OCT at the basic dose (10 μg/kg) under the same HPLC conditions (data not shown). The HPLC profile of non-polar metabolites after administration of OCT is shown in Fig. 2. Under these HPLC conditions P5 and P8 each gave a single peak, respectively. However, it is suggested that P6 and P7 could contain more than three metabolites in each peak after comparison of the t_R with several synthetic putative metabolites. Rechromatography of P6 and P7 by normal phase HPLC was carried out (Fig. 3). The 'rechromatogram' of P6 gave a further four major peaks (P6-1, P6-2, P6-3 and P6-4). It was also shown that the t_R's of P6-2, P6-3 and P6-4 were identical to those of 20*S*(OH)-hexanor-OCT, (25*S*)-26(OH)OCT and (25*R*)-26(OH)OCT, respectively. Similarly, the 'rechromatogram' of P7 gave a further three peaks (P7-1, P7-2 and P7-3). It was shown that the t_R of P7-2 was identical to that of both 24*R*(OH)OCT and 24*S*(OH)OCT, which were not separated by normal phase HPLC (despite showing a good separation on reverse phase HPLC). There was no significant peak which coincided with the t_R's of 20oxo-hexanor-OCT. The t_R's of P6-1, P7-1 and P7-3 were not identical to any of the synthetic putative metabolites.

GC-MS of the extract of plasma metabolites

Side-chain cleavage metabolites (I-1, I-2, I-3); Examination of side-chain cleavage metabolites such as 20*R*(OH)-hexanor-OCT, 20*S*(OH)-hexanor-OCT and 20oxo-hexnor-OCT was carried out using the mass chromatogram of the molecular ions and some unique fragment ions (Fig. 4), which had previously been examined [19]; (a) *m/z* 548, 458, 368 and 117 for the TMS derivatives of 20*R*(OH)-hexanor-OCT and 20*S*(OH)-hexanor-OCT and (b) *m/z* 474, 384 and 294 for the TMS derivative of 20oxo-hexnor-OCT. In the mass chromatogram shown in Fig. 4(b), three peaks were detected at which these four ions were eluted together (I-1, I-2 and I-3). From a comparison with synthetic compounds, these t_R's were not identical to those of 20*R*(OH)-hexanor-OCT, but were identical to those of 20*S*(OH)-hexanor-OCT. Both these compounds are confirmed to give rise to three thermal-isomerization products for each compound during GC analysis [19]. Fig. 5(A) shows the GC-MS spectra of the first peak (I-1). The mass spectrum was confirmed to be almost completely identical to that of the TMS derivative of 20*S*(OH)-hexanor-OCT. The mass spectra of the second and third peaks (I-2 and I-3) also coincided with those of the TMS derivative of 20*S*(OH)-hexanor-OCT. We conclude that the metabolite giving these three peaks is 20*S*(OH)-hexanor-OCT. On the other hand, the TMS derivative of 20oxo-hexanor-OCT was not detected in the mass chromatogram Fig. 4(a). This result is consistent with the evidence obtained from rechromatography of P7 [Fig. 3(B)]. Therefore, we conclude that there is very little 20oxo-hexanor-OCT among the plasma metabolites.

Side-chain oxidation metabolites (II-1, II-2, II-3, II-4, II-5); Side-chain oxidation metabolites such as 24*R*(OH)OCT, 24*S*(OH)OCT, (25*R*)-26(OH)OCT, (25*S*)-26(OH)OCT and 24-oxoOCT were examined using the mass chromatogram of the molecular ions and unique fragment ions for each compound (Fig. 4); (c) *m/z* 648, 558 and 517 for 24-oxoOCT, (d) *m/z* 722,632, 591 and 145 for TMS derivatives of (25*R*)-26(OH)OCT, (25*S*)-26(OH)OCT and (e) *m/z* 722, 632, 591 and 131 for TMS derivatives of 24*R*(OH)OCT and 24*S*(OH)OCT.

In the mass chromatograms Fig. 4(e), four peaks in which the four examined ions eluted together were detected (II-1, II-2, II-4 and II-5). The t_R's of II-1 and II-4 were identical to those of the TMS derivative of 24*R*(OH)OCT and the t_R's of II-2 and II-5 coincided with those of the TMS derivative of 24*S*(OH)OCT. GC-MS spectra of II-1 and II-2 are shown in Fig. 5(B) and Fig. 5(C), respectively. Both gave very similar mass spectra and the mass spectra of II-1 and II-2 were confirmed to be virtually identical to those for the TMS derivatives of the synthetic 24*R*(OH)OCT and 24*S*(OH)OCT, respectively. Similarly, the mass spectra of II-4 and II-5 which are regarded as thermal-isomerization products, also gave a similar spectrum to the corresponding isomers, II-1 and II-2, respectively. From these data, we conclude that the metabolite giving II-1 and II-4 is 24*R*(OH)OCT and the metabolite giving II-2 and II-5 is 24*S*(OH)OCT.

In the mass chromatograms of Fig. 4(d), a weak peak was detected at which the four ions eluted together (II-3). The t_R's of II-3 were identical to the first t_R of the TMS derivatives of (25*R*)-26(OH)OCT and (25*S*)-26(OH)OCT, which were confirmed not to be chromatographed under the GC conditions used. Although the TMS derivatives of (25*R*)-26(OH)OCT and (25*S*)-26(OH)OCT also give rise to two thermal-isomerization products each [19], we could not detect the second peak in the mass chromatograms obtained from plasma extracts due, presumably, to the very small amount present. The GC-MS

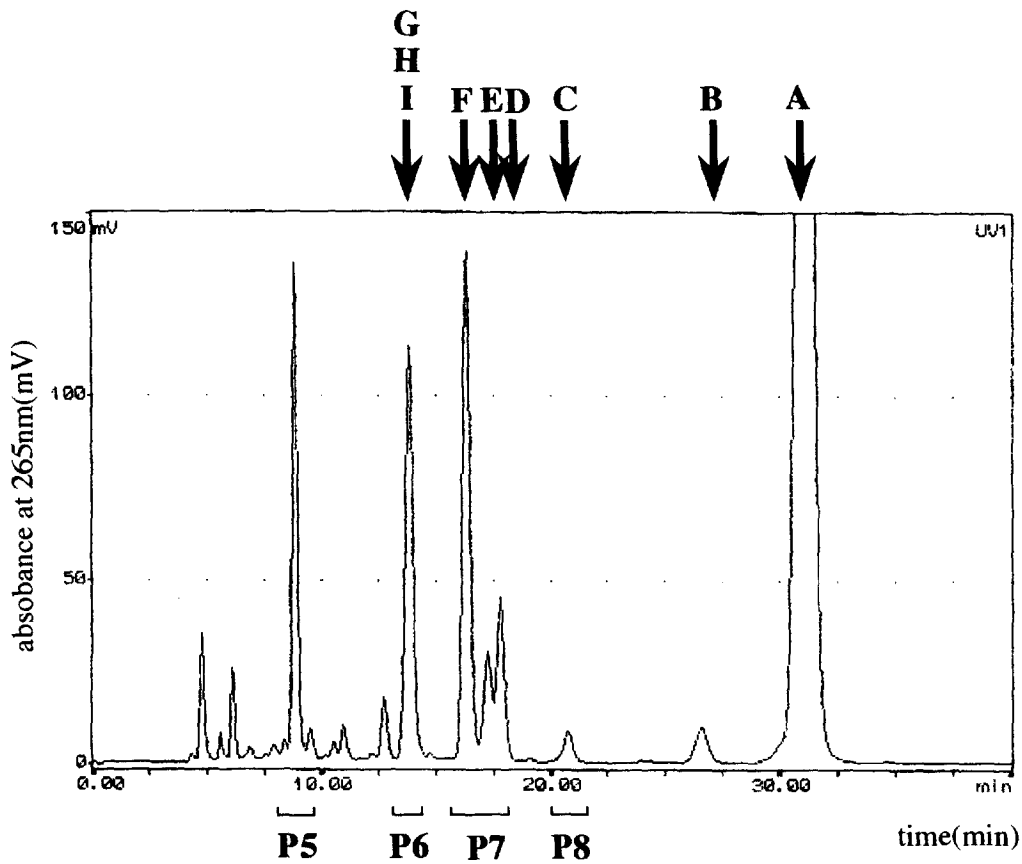

Fig. 2. High performance liquid chromatographic profile of the extracts of plasma metabolites 2 h after administration of OCT to rats. Arrows (A to I) indicate the retention times of synthetic standards in the same system; (A) OCT, (B) pre-OCT, (C) 24-oxoOCT, (D) 20oxo-hexanor-OCT, (E) 24*S*(OH)OCT, (F) 24*R*(OH)OCT, (G) 20*S*(OH)-hexanor-OCT, (H) (25*R*)-26(OH)OCT and (I) (25*S*)-26(OH)OCT. Fraction numbers (P5 to P8) show the isolation periods of metabolites for further analysis. High performance liquid chromatography was carried out under the following conditions; column: YMC-Pack ODS-A A-313 (6.0 × 250 mm), mobile phase: H_2O–THF–CH_3CN (65:35:2, v/v/v), flow rate: 1.0 ml/min, detection: UV 265 nm.

spectra of II-3 [Fig. 5(D)] was found to coincide almost exactly with those of the TMS derivatives of (25*R*)-26(OH)OCT and (25*S*)-26(OH)OCT which exhibited almost the same mass spectra. From the GC-MS data and HPLC 'rechromatogram' of P6 [Fig. 3(A)], we concluded that the metabolites giving II-3 are a mixture of (25*R*)-26(OH)OCT and (25*S*)-26(OH)OCT.

However, very little TMS derivative of the 24-oxoOCT was detected in the mass chromatogram Fig. 4(c). Therefore, we tried to perform an identification by LC-MS which has a higher sensitivity than GC-MS [19].

Identification of P8 by LC-MS

The LC-MS APCI mass spectrum of P8 isolated from plasma is shown in Fig. 6. P8 eluted at approximately 11.5 min, which is an almost identical t_R to that of authentic 24-oxoOCT [19]. The mass spectrum gave signals reflecting the intact analyte (*m/z* 450, 433 and 415) and fragment ions (*m/z* 315, 297 and 279), which were found to be virtually identical to that of synthetic 24-oxoOCT. We conclude that P8 is 24-oxoOCT.

Interpretation of the structure of P5

The GC-MS spectrum of the TMS derivative of P5 isolated from plasma is shown in Fig. 7. The TMS derivative of P5 gave a molecular ion of *m/z* 564, suggesting it to be 16 amu greater than the molecular ion of 20*S*(OH)-hexanor-OCT. In addition, a prominent fragment ion was observed at m/z 117 corresponding to a C2-fragment from C-20 and C-21 bearing a TMS group, as in the case of 20*S*(OH)-hexanor-OCT. The other fragment ions at m/z 429, 339, 249 and 217 corresponded to M-117-H_2O, M-117-TMSOH-H_2O, M-117-2TMSOH-H_2O and loss of a fragment containing carbon C1, C2 and C3, respectively. This interpretation suggests that P5 is a metabolite which has an oxygen atom at C or D ring in the vitamin D_3 skeleton. Interestingly, the new hydroxy group could not be converted to a TMS derivative. This evidence suggests the possibility that the new hydroxy position might be vicinal (C17) to a

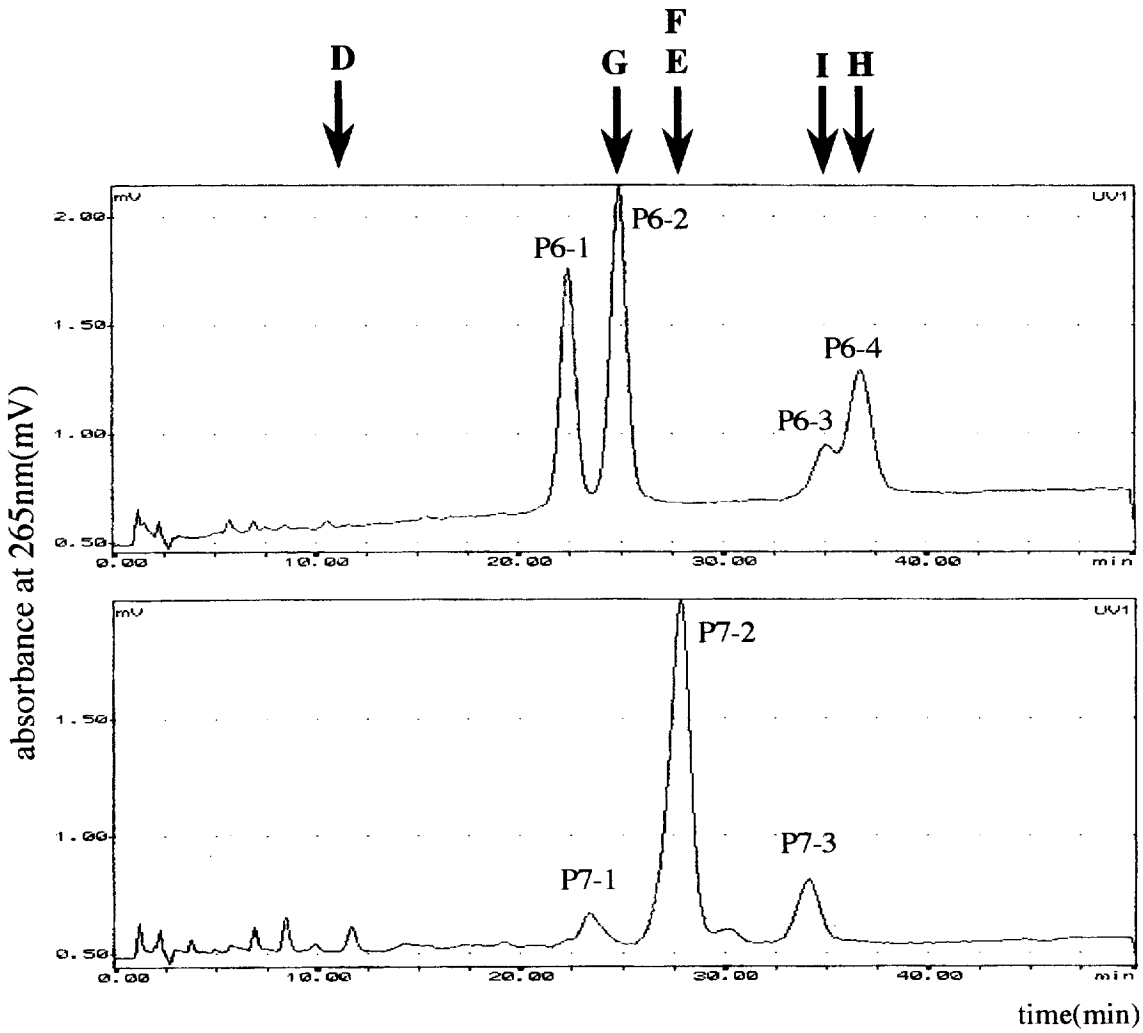

Fig. 3. High performance liquid chromatographic profile of P6 (upper panel) and P7 (lower panel). Arrows (D to I) indicate the retention times of synthetic standards in the same system; (D) 20oxo-hexanor-OCT, (E) 24*S*(OH)OCT, (F) 24*R*(OH)OCT, (G) 20*S*(OH)-hexanor-OCT, (H) (25*R*)-26(OH)OCT and (I) (25*S*)-26(OH)OCT. High performance liquid chromatography was carried out under the following conditions; column: CAPCEL PAK NH_2 (4.6 × 250 mm), mobile phase: hexane–isopropanol–methanol (91:7:2, v/v/v), flow rate: 2.5 ml/min, detection: UV 265 nm.

hydroxy group which results in steric hindrance [21–24]. In order to confirm this speculation, we analyzed the periodate cleavage product of P5 by LC-MS. The periodate cleavage product of P5 eluted at an almost identical t_R to that of the synthetic putative product, 17oxo-octanor-OCT. Fig. 8 shows the LC-MS APCI mass spectra of the periodate cleavage product and 17oxo-octanor-OCT. The periodate cleavage product of P5 gave some prominent ions reflecting the intact analyte at *m/z* 320, 303 and 285 corresponding to $[M + NH_4]^+$, $[M + H]^+$ and $[M + H–H_2O]^+$, respectively. This spectrum was found to be virtually identical to that of the synthetic 17oxo-octanor-OCT. We conclude that P5 is 17,20*S*$(OH)_2$-hexanor-OCT.

DISCUSSION

The identification of plasma metabolites after intravenous administration of OCT to rats was carried out using methods established previously by GC-MS and LC-MS, which enable us to examine almost all the metabolites without isolation by HPLC [19]. Seven metabolites were identified, including a new type of 17-hydroxy metabolite for vitamin D_3 and its analogues. Kobayashi *et al.* [15] demonstrated that OCT mainly circulates in the blood in its intact form, non-specifically bound to lipoproteins, after intravenous administration of OCT to rats and is finally excreted in the bile as a glucuronide of 20*S*(OH)-hexanor-

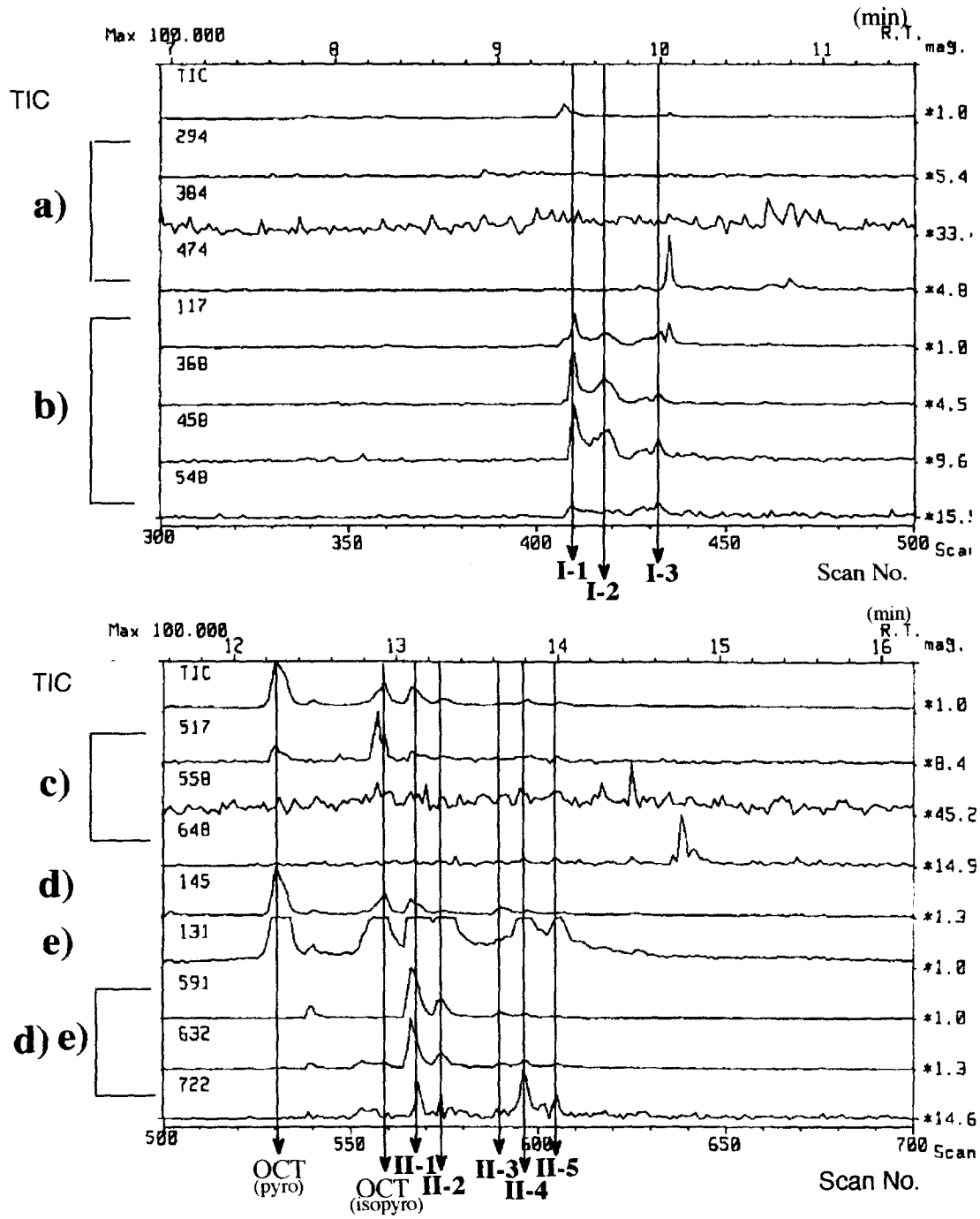

Fig. 4. Mass chromatograms following gas chromatography-mass spectrometry of pertrimethylsilyl ethers of metabolites extracted from plasma after administration of OCT. The unique ions for the pertrimethylsilyl ethers of the synthetic postulated metabolites were monitored as selected ions to screen the metabolites: (a) 20oxo-hexanor-OCT (*m/z* 474, 384, 294), (b) 20*R*(OH)-hexanor-OCT or 20*S*(OH)-hexanor-OCT (*m/z* 548, 458, 368, 117), (c) 24-oxoOCT (*m/z* 648, 558, 517), (d) (25*R*)-26(OH)-OCT or (25*S*)-26(OH)-OCT (*m/z* 722, 632, 591, 145) and (e) 24*R*(OH)OCT or 24*S*(OH)OCT (*m/z* 722, 632, 591, 131).

OCT. We also confirmed that almost all the radioactivity in plasma 1 h after administration of [2β-^{3}H]OCT was unchanged OCT (data not shown). However, for the plasma metabolites at 2 h, more than half the total radioactivity in plasma was due to metabolites, suggesting that some metabolites as well as unchanged OCT also circulate in the blood 1 h to 2 h after administration of OCT.

We propose a possible metabolic pathway for OCT in rats in Fig. 9. A comparison with the proposed metabolic pathway for OCT in cell cultures [13] showed some similarities and differences. The side-chain oxidation pathways *in vivo* such as 24(OH)OCT and 26(OH)OCT showed a similar pattern to that in cell cultures except for the presence of 24-oxoOCT. The identification of 24-oxoOCT in

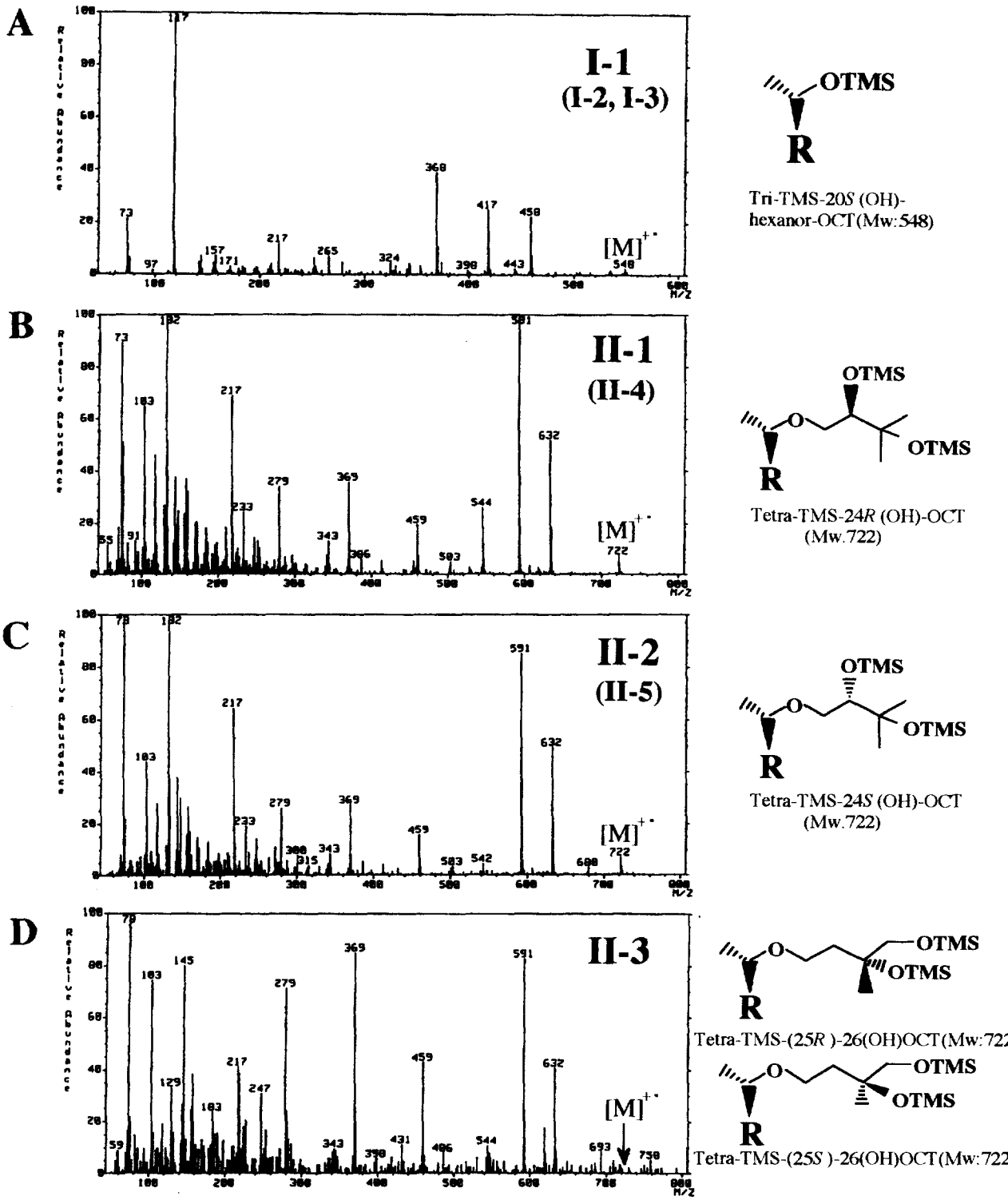

Fig. 5. Gas chromatography-mass spectra of pertrimethylsilyl-ethers of plasma metabolites (I-1, II-1, II-2 and II-3). Mass spectra were obtained by gas chromatography-mass spectrometer (DX-300, JEOL) after extraction of metabolites and pertrimethylsililation.

plasma might be significant as far as the pharmacological effect of OCT *in vivo* is concerned, because it has shown antiproliferative activity towards human promyelocytic leukemia cells (HL-60 cells) comparable to that of OCT [17]. The side-chain oxidation pathways of OCT were virtually identical to those of 1,25-$(OH)_2D_3$ as described previously [25–27]. The fact that there was much more 24*R*(OH)OCT in plasma than 24*S*(OH)OCT and 24-oxoOCT (24*R*≫24*S*≒24oxo) was similar to 1,25-$(OH)_2D_3$ in

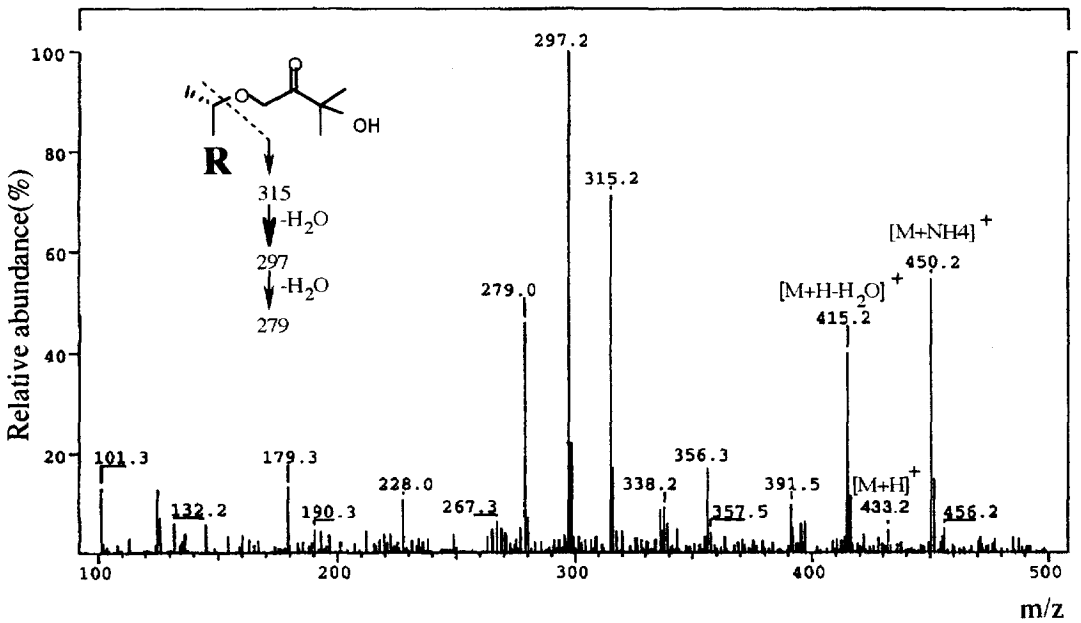

Fig. 6. Liquid chromatography-mass spectrum (APCI) of putative 24-oxoOCT (P8, Fig. 2). P8 was isolated from plasma after administration of OCT by the procedure described in Section 2.

dogs [27]. This evidence suggests that 24*S*(OH)OCT is mainly synthesized in the body via 24R(OH)OCT to 24-oxoOCT, following a pathway proposed by Ishizuka *et al.* (Fig. 9) [27]. On the other hand, the side-chain cleavage pathways showed a different metabolic pattern from that of cell cultures. Both 20oxo-hexanor-OCT, which was detected as the main and final metabolite in hepatoma cells, and 20*R*(OH)-hexanor-OCT were not detected as plasma metabolites. Furthermore, 17,20*S*(OH)$_2$-hexanor-OCT, which was identified as one of the main plasma metabolites, has not been detected in any cell culture models. This evidence suggests that 20*S*(OH)-hexanor-OCT produced from OCT or other SCOMs, which is presumably formed from an unstable hemiacetal compound via carbon-23 hydroxylation, undergoes further metabolism to form 17,20*S*(OH)$_2$-hexanor-OCT and a glucuronide of 20*S*(OH)-hexanor-OCT *in vivo*. On the contrary, 20*S*(OH)-hexanor-OCT and/or 20*R*(OH)-hexanor-OCT formed in cell cultures, undergoes further oxidation to 20-oxo-hexanor-OCT predominantly, because in cell cultures it is not easily metabolized to the glucuronide of 20*S*(OH)-hexanor-OCT as well as 17,20*S*(OH)$_2$-hex-

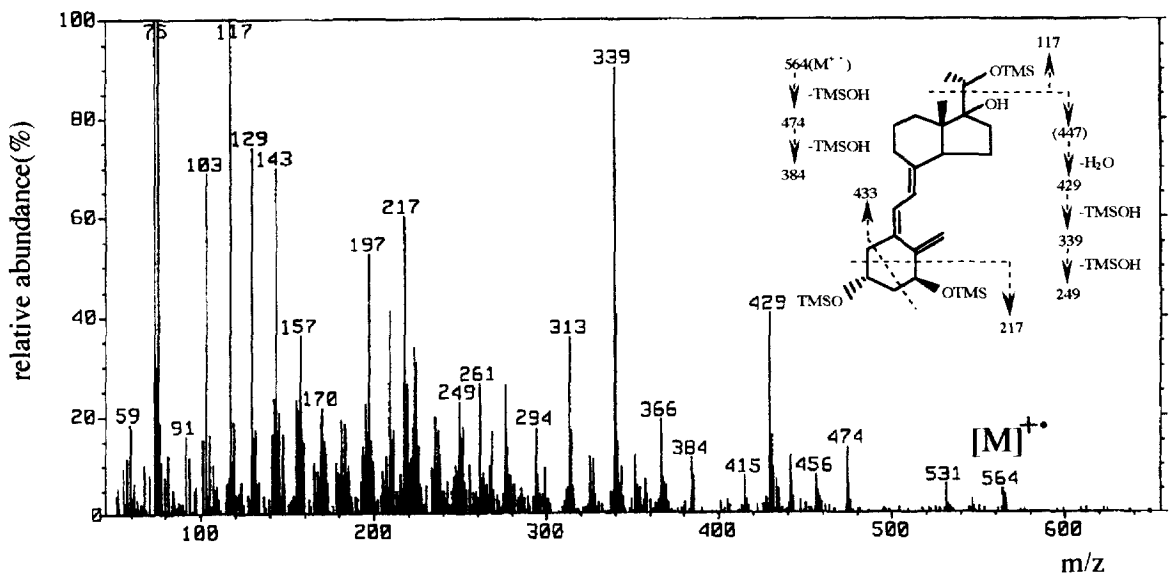

Fig. 7. Gas chromatography-mass spectrum of the pertrimethylsilyl-ether of P5

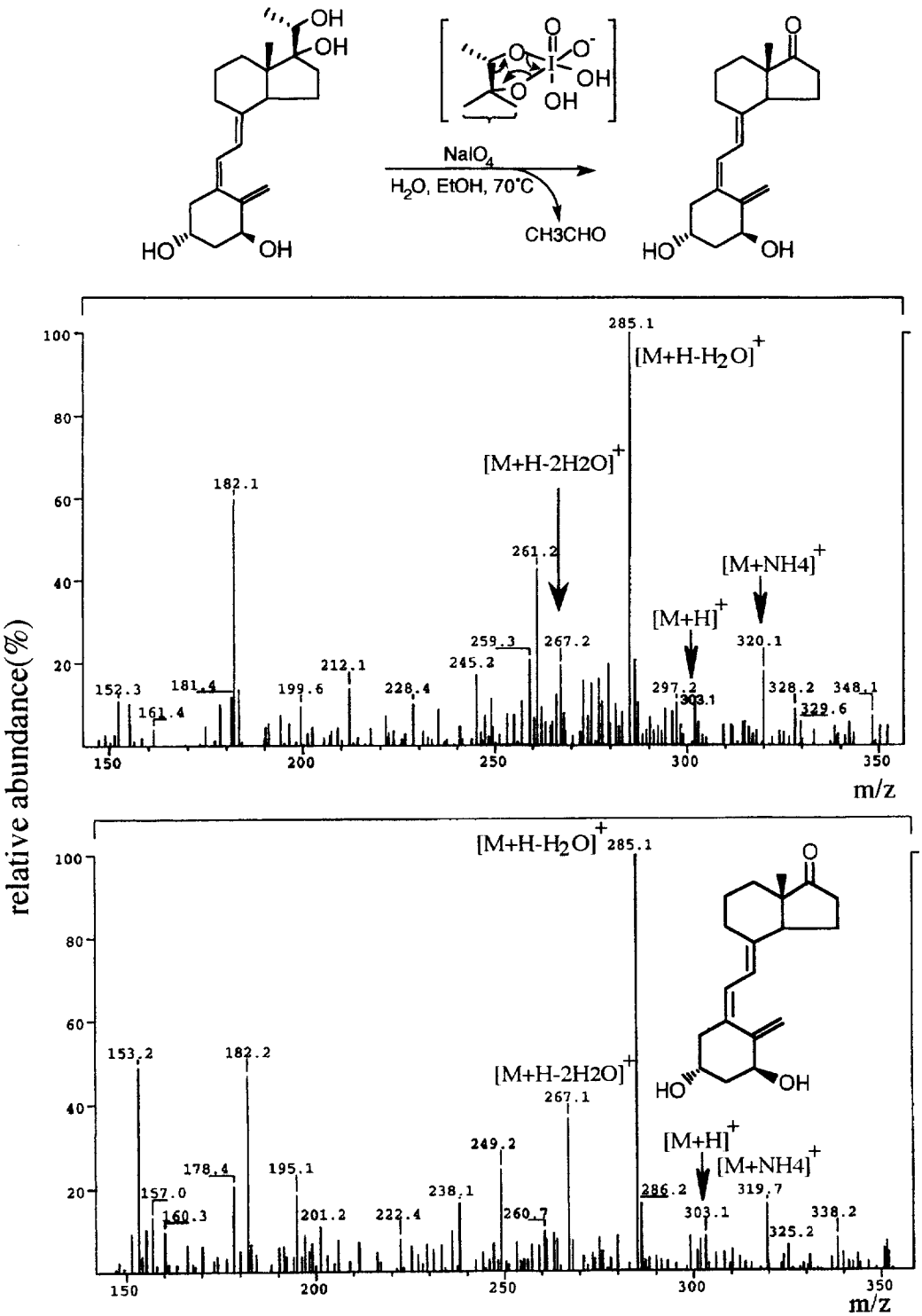

Fig. 8. Liquid chromatography-mass spectra (APCI) of the periodate cleavage product of P5 (upper panel) and the synthetic 17oxo-octanor-OCT (lower panel).

anor-OCT. From differences in the metabolism of OCT *in vivo* and in cell culture models, it is suggested that vitamin D-target cell lines reflect a common metabolism like oxidation of the vitamin D_3 side-chain as described previously [28–30]. However, it is difficult to mimic all pathways of metabolism associated with the modified position and the proximity in the side-chain of the analogues.

Although there is little information on the formation and further metabolism of 17,20*S*(OH)$_2$-hexanor-OCT so far, we speculate that it is formed from 20*S*(OH)-hexanor-OCT and then excreted as

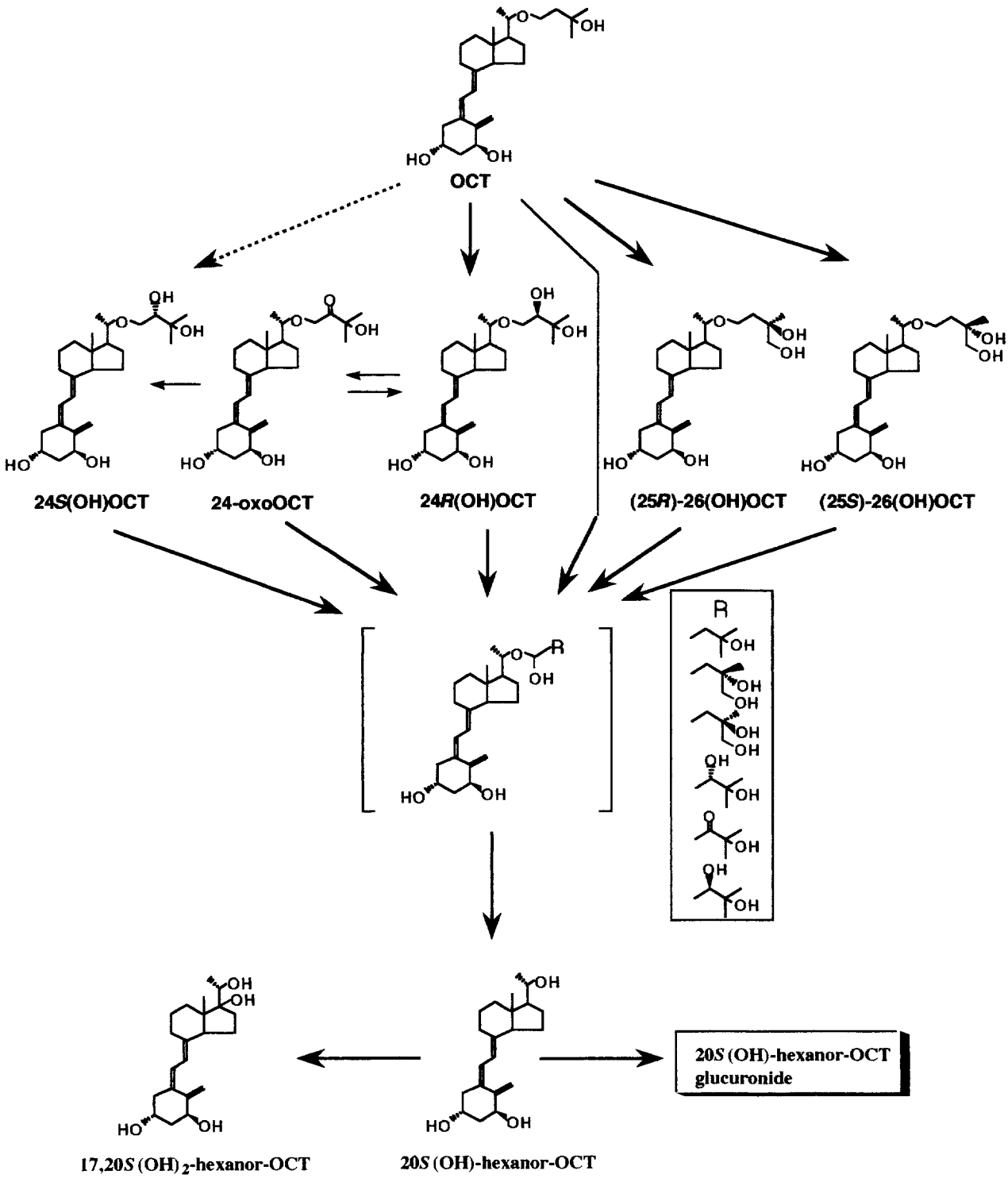

Fig. 9. Postulated metabolic pathway of OCT in rats.

polar metabolites. A carbon-17 hydroxylation involving seco-steroids such as vitamin D_3 and its analogues is an unusual pathway which has never been reported. However, the hydroxylation of steroids, such as the biotransformation of progesterone to a 17α-hydrocorticoid mediated by 17α-hydroxylase, is a common metabolic pathway [31–34]. The carbon-17 hydroxylation of OCT might be caused by the unique metabolic pathway of OCT, namely, cleavage of the side-chain between carbon-23 (C_{23}) and oxygen-22 (O_{22}). It has been reported that side-chain oxidation metabolites such as 20*S*(OH)-hexanor-OCT, 20*R*(OH)-hexanor-OCT and 20-oxo-hexnor-OCT markedly lower the vitamin D_3 receptor binding

affinity and the cell growth of human promyelcytic leukemic cells (HL-60 cells) as compared with those of OCT and side-chain oxidation metabolites [13]. Therefore, the 17,20*S*$(OH)_2$-hexanor-OCT itself is considered to have little biological activity. However, the unique metabolic pathway (17-hydroxylation and cleavage of the C_{23}–O_{22} bond) and the rate of metabolism might play an important role in the unique properties of OCT, such as its lack of hyper-calcemic activity.

The structure of the polar (water soluble) metabolites as well as a couple of the non-polar metabolites remain unclear. Almost all polar metabolites are suggested to have no side-chain from a comparison of the two HPLC radio-chromatograms of the plasma metabolites obtained from [2β-^{3}H]OCT and [26-^{3}H]OCT. Also they may be artifacts which are associated with the free-^{3}H released from the D-ring of OCT, enzymatically or non-enzymatically. The detailed elucidation of their structure is under investigation.

REFERENCES

1. Abe J., Miyaura C., Sakagami H., Takeda M., Konno K., Yamazaki T., Yoshiki S. and Suda T., Differentiation of mouse myeloid leukemia cells induced by 1α,25-dihydroxyvitamin D_3. *Proc. Natl. Acad. Sci. U.S.A.* **78** (1981) 4990–4994.
2. Osterm V. K. and Deluka H. F., The vitamin D-induced differentiation of HL-60 cells: structural requirements. *Steroids* **49** (1987) 73–102.
3. Kubodera N., Miyamoto K., Akiyama M., Matsumoto M. and Mori T., Synthetic studies of vitamin D analogues. IX. Synthesis and differentiation-inducing activity of 1α,25-dihydroxy-23-oxa-, thia- and azavitamin D3. *Chem. Pharm. Bull.* **39** (1991) 3221–3224.
4. Kubodera N., Watanabe H., Kawanishi T. and Matsumoto M., Synthetic studies of vitamin D analogues. XI. Synthesis and differentiation-inducing activity of 1α,25-dihydroxy-22-oxa-vitamin D_3 analogues. *Chem. Pharm. Bull.* **40** (1992) 1494–1499.
5. Brown, A. J., Dusso, A. and Raisz, L. G., *Vitamin D. Gene Regulation, Structure–Function Analysis and Clinical Application*, eds. A. W. Norman, R. Bouillon, M. Thomasset. Walter de Gruyter, Berlin and New York, 1991, pp. 289–297.
6. Jones G. and Calverley M. J., A dialogue on analogues newer vitamin-D drugs for use in bone disease, psoriasis, and cancer. *Trends Endocrinol. Metab.* **3** (1993) 297–303.
7. Murayama E., Miyamoto K., Kubodera N., Mori T. and Matsunaga I., Synthetic studies of vitamin D3 analogues. VIII. Synthesis of 22-oxavitamin D_3 analogues. *Chem. Pharm. Bull.* **34** (1986) 4410–4413.
8. Abe J., Morikawa M., Miyamoto K., Kaiho S., Fukushima M., Miyaura C., Abe E., Suda T. and Nishii Y., Synthetic analogues of vitamin D_3 with an oxygen atom in the side chain skeleton. *FEBS Lett.* **226** (1987) 58–62.
9. Abe J., Takita Y., Nakano T., Miyaura C., Suda T. and Nishii Y., A synthetic analogue of vitamin D3, 22-oxa-1α,25-dihydroxyvitamin D_3, is a potent modulator of *in vitro* immunoregulating activity without inducing hypercalcemia in mice. *Endocrinology* **124** (1989) 2645–2647.
10. Brown A. J., Ritter C. R., Fench J. L., Morrissey J., Martin K. J., Murayama E., Nishii Y. and Slatopolsky E., The noncalcemic analogue of vitamin D, 22-oxacalcitriol, suppresses parathyroid hormone synthesis and secretion. *J. Clin. Invest.* **84** (1989) 728–732.
11. Takigawa M., Fallon M., Stein B. and Epstein S., The effect of a new vitamin D analog, 22-oxa-1α,25$(OH)_2D_3$, on bone mineral metabolism in normal male rats. *Calcif. Tissue Int.* **50** (1992) 521–523.
12. Brown A. J., Berkoben M., Ritter C., Kubodera N., Nishii Y. and Slatpolsky E., Metabolism of 22-oxacalcitriol by a vitamin D-inducible pathway in cultured parathyroid cells. *Biochem. Biophys. Res. Commun.* **147** (1992) 565–571.
13. Masuda S., Byford V., Kremer R., Makin H. L. J., Kubodera N., Nishii Y., Okazaki A., Okano T., Kobayashi T. and Jones G., *In vitro* metabolism of the vitamin D analog, 22-oxacalcitriol, using cultured osteosarcoma, hepatoma and keratinocyte cell lines. *J. Biol. Chem.* **271** (1996) 8700–8708.
14. Kobayashi, T., Okano, T., Tsugawa, N., Masuda, S., Takeuchi, A. and Nishii, Y., Calcium-regulation hormone. II. Calcium transport, bone metabolism and new drugs. In *Contrib. Nephrol.*, ed. H. Morii. Basel Karger, Switzerland, 1991, pp. 129–133.
15. Kobayashi T., Tsugawa N., Okano T., Masuda S., Takeuchi A., Kubodera N. and Nishii Y., The binding properties, with blood proteins, and tissue distribution of 22-oxa-1α,25-dihydroxyvitamin D_3, a noncalcemic analogue of 1α,25-dihydroxyvitamin D_3, in rats. *J. Biochem.* **115** (1994) 373–380.
16. Kubodera N., Watanabe H., Hatakeyama S., Tazumi K. and Takano S., Synthesis of postulated metabolites of 1α,25-dihydroxy-22-oxa-vitamin D_3. *Bioorg. Med. Chem. Lett.* **4** (1994) 753–756.
17. Watanabe H., Hatakeyama S., Tazumi K., Takano S., Masuda S., Okano T., Kobayashi T. and Kubodera N., Synthetic studies of vitamin D analogs. XXII. Synthesis and antiproliferation activity of putative metabolites of 1α,25-dihydroxy-22-oxavitamin D_3. *Chem. Phram. Bull.* **44** (1996) 2280–2286.
18. Watanabe H., Akiyama M., Kawanishi T. and Kubodera N., Synthesis of tritiated 1α,25-dihydroxy-22-oxavitamin D_3. *J. Labeled Comp. Radiopharm.* **36** (1995) 645–654.
19. Ishigai M., Ishitani Y. and Kumaki K., Characteristics of mass spectrometric analyses coupled to gas chromatography and liquid chromatography for 22-oxacalcitriol, an analog of 1α,25-dihydroxy-vitamin D_3 and related compounds. *J. Chromatogr. B* **704** (1997) 11–17.
20. Nair P. P., Bucana C., Leon S. D. E. and Turner D. A., Gas chromatographic studies of vitamin D_2 and D_3. *Anal. Chem.* **37** (1965) 631–636.
21. Miyazaki H., Ishibashi M., Itoh M. and Yamashita K., Diethylsilyl ether and diethylsiliconide derivatives in gas chromatography mass spectrometry of hydroxylated steroids. *Biomed. Mass Spectrom.* **11** (8) (1984) 377–382.
22. Nakata H., Ishibashi M., Itoh M. and Miyazaki H., Diethylhydrogensilyl cyclic diethylsilylene derivatives in gas chromatography/mass spectrometry of hydroxylated steroids. *Org. Mass Spectrom.* **22** (1987) 23–29.
23. Ishibashi M., Itoh M., Yamashita K., Miyazaki H. and Nakata H., Diethylhydrogensilyl cyclic diethylsilylene derivatives in gas chromatography-mass spectrometry of hydroxylated steroids. II. *Chem. Pharm. Bull.* **34** (1986) 3298–3305.
24. Ishibashi M., Irie T. and Miyazaki H., Diethylhydrogensilyl-cyclic diethylsililene derivatives in the gas chromatography-mass spectrometry of hydroxylated steroids. IV. Hydrocortizone. *J. Chromatogr.* **399** (1987) 197–206.
25. Reinhardt T. A., Napoli J. L., Beitz D. C., Littledike E. T. and Horst R. L., 1,24,25-Trihydroxyvitamin D_3: A circulating metabolite in vitamin D_3-treated bovine. *Arch. Biochem. Biophys.* **213** (1982) 163–168.
26. Reinhardt T. A., Napoli J. L., Praminic E., Littledike E. T., Beitz D. C., Partridge J. J., Uskokovic M. R. and Horst R. L., 1α,25,26-Trihydroxy vitamin D_3: An *in vivo* and *in vitro* metabolite of vitamin D_3. *Biochemistry* **20** (1981) 6230–6235.
27. Ishizuka S., Ishimoto S. and Norman A. W., Isolation and Identification of 1α,25-dihydroxy-24-oxovitamin D_3, 1α,25-dihydroxyvitamin D_3 26,23-lactone, and 1α,24(S),25-trihydroxyvitamin D_3: *In vivo* metabolites of 1α,25-dihydroxyvitamin D_3. *Biochemistry* **23** (1984) 1473–1478.
28. Lohnes D. and Jones G., Side chain metabolism of vitamin D3 in osteosarcoma cell line UMR-106. *J. Biol. Chem.* **262** (1987) 14394–14401.
29. Henderson J., Sebag M., Rhim J., Goltzman D. and Kremer R., Dysregulation of parathyroid hormone-like peptide ex-

pression and secretionin a keratinocyte model of tumor progression. *Cancer Res.* **51** (1991) 6521–6528.

30. Masuda S., Strugnell S., Calverley M., Makin H. L. J., Kremer R. and Jones G., *In vitro* metabolism of the anti-psoriatic vitamin D analog, capcipotriol, in two cultured human keratinocyte models. *J. Biol. Chem.* **269** (1994) 4794–4803.
31. Matsumoto K., Mahajan D. K. and Samuels L. T., The influence of progesterone on the conversion of 17-hydroxyprogesterone to testosterone in the mouse testis. *Endocrinology* **94** (1974) 808–814.
32. Nakajin S., Shimoda M., Haniu M., Shivery J. E. and Hall P. F., C21 steroids side chain cleavage enzyme from porcine adrenal microsomes. *J. Biol. Chem.* **259** (1984) 3971–3976.
33. Zuber M. X., Shimpson E. R. and Waterman M. R., Expression of bovine 17α-hydroxylase cytochrome P-450 cDNA in non-steroidgenic (Cos 1) cells. *Science* **234** (1986) 1258–1261.
34. Imai T., Globerman H., Gerner J. M., Kagawa N. and Waterman M. R., Expression and purification of functional human 17α-hydroxylase/17,20-lyase (P450c17) in *Escherichia coli*. *J. Biol. Chem.* **268** (1993) 19681–19689.